

See discussions, stats, and author profiles for this publication at: <https://www.researchgate.net/publication/234881083>

# Lock-in common-mode rejection demodulation: Measurement technique and applications to thermal-wave detection. Experimental

ARTICLE *in* REVIEW OF SCIENTIFIC INSTRUMENTS · MAY 2000

Impact Factor: 1.61 · DOI: 10.1063/1.1150634

---

CITATIONS

11

---

READS

28

3 AUTHORS, INCLUDING:



[Andreas Mandelis](#)

University of Toronto

522 PUBLICATIONS 6,168 CITATIONS

SEE PROFILE

# Lock-in common-mode rejection demodulation: Measurement technique and applications to thermal-wave detection: Theoretical

Andreas Mandelis,<sup>a)</sup> Stefano Paoloni,<sup>b)</sup> and Lena Nicolaidis

*Photothermal and Optoelectronic Diagnostics Laboratories, Department of Mechanical and Industrial Engineering, University of Toronto, and Materials and Manufacturing Ontario, Toronto M5S 3G8, Canada*

(Received 23 November 1999; accepted for publication 22 February 2000)

The ability of conventional single-ended photothermal techniques to detect weak inhomogeneities in a given material is mainly limited by two instrumental factors: the signal-to-noise ratio (SNR) and the amplitude dynamic range. The amplitude level is limited by the output signal baseline, and may be too high to monitor relatively small variations introduced by the presence of weak inhomogeneities. The purpose of this work is to introduce a novel photothermal signal generation methodology, the principle of which can be broadly applied to any technique utilizing a lock-in analyzer demodulation scheme of periodic signal wave forms. Unlike the conventional single-ended periodic excitation wave form, which uses a 50% duty-cycle square wave or sinusoidal modulation of the pump laser heating beam, a more complicated periodic modulation wave form is employed, resulting in the equivalent of differential-signal demodulation. The new wave form takes advantage of the real-time differential action performed by the lock-in amplifier weighing function over the two half periods of the modulated signal. This results in enhanced signal dynamic range due to the efficient suppression of the baseline and a substantial improvement in the SNR. The main features of this technique are investigated with a theoretical model for an arbitrary repetitive signal wave form and, in particular, for a photothermal signal. The dependence of the signal on the wave form parameters is also discussed. © 2000 American Institute of Physics. [S0034-6748(00)03106-3]

## I. INTRODUCTION

Photothermal techniques have been established for many years as a tool for non-destructive evaluation of material properties.<sup>1</sup> Thermophysical properties are, in general, an indicator of the degree of homogeneity of a given sample because they are strongly affected by variations occurring in the sample microstructure. Briefly, the common working principle of conventional photothermal techniques is based on the study of the periodic temperature distribution, i.e., the thermal wave, produced in a given sample as a result of heating due to an intensity modulated pump laser source impinging on the surface. Thermal waves inside a homogeneous sample diffuse over a characteristic distance, which is given by the thermal diffusion length  $\sqrt{D/\pi f}$ , where  $D$  is the thermal diffusivity and  $f$  the modulation frequency. By changing the modulation frequency, the thermal wave propagates over different distances and probes the presence of thermal inhomogeneities located at different depths beneath the surface. In fact, thermal features inside the sample alter the heat transfer rate thus affecting the resulting surface temperature distribution, which is detected by various photothermal techniques. Finally, by analyzing the dependence of the photothermal signal on the modulation frequency, it is possible to derive some material parameters (thermal diffusivity, conductivity) and/or obtain information on inhomogeneities,

such as position, size, depth, profile, etc. This is the basic principle of all thermal wave inspection methods.

Conventional frequency domain photothermal methods are basically single-ended techniques meaning that a 50% duty-cycle square wave, or a sinusoidal wave is used for modulating the heating beam intensity along with a lock-in amplifier (LIA) for signal processing. The implications of single-ended detection are that, if the signal contributions from sample inhomogeneities are much smaller than that from the homogeneous bulk of the material (background signal), then they cannot be easily detected. In a single-ended technique the sensitivity of the experiment is determined by the magnitude of the background signal. Without further conditioning, the signal level is simply too high to probe variations of amplitude much smaller than this background. In this work, these very small variations are called “contrast signals.”

In order to obtain quantitative information about the sample properties, the photothermal signal must be compared to that obtained from a homogeneous reference sample in order to account for the instrumental transfer function. Properly normalized signal amplitude ratios and phase differences must be collected as a function of the modulation frequency. This procedure introduces several problems especially when one intends to probe slightly inhomogeneous samples with theoretical contrast signals approaching the noise level of the experiment. In fact, the effect of normalization is, in general, to add some more noise to the measurement, thus resulting in poorer signal-to-noise ratio (SNR), which usually masks contrast signals. Despite the

<sup>a)</sup>Author to whom correspondence should be addressed; electronic mail: mandelis@mie.utoronto.ca

<sup>b)</sup>On leave from INFN-Universita' di Roma “La Sapienza,” Dipartimento di Energetica Via Scarpa 16, 00161 Roma, Italy.

advantage of the narrow-bandwidth filtering action of the demodulating LIA a strong noise reduction is required for these kinds of applications and conventional photothermal techniques do not compensate against slowly varying drift phenomena, which can occur during a measurement, because of their single-ended nature.<sup>2</sup> The noise frequency components within the narrow filter bandwidth are not rejected and are still present in the output signal.

In this article we introduce a lock-in common-mode rejection demodulation signal methodology as an alternative to the single-ended techniques. This signal generation scheme, when coupled to a photothermal detection system is, in principle, capable of detecting very weak inhomogeneities in materials that are not possible to detect with conventional techniques. It should be noted that the new signal generation and detection scheme introduced in this article can be readily used with any physical detection principle involving signal demodulation. Our choice of a photothermal system paradigm reflects a “worst-case” scenario due to the relatively poor SNR of thermal-wave signals compared to optical or electrical techniques.

## II. COMMON-MODE REJECTION WAVE FORM DESIGN

The basic idea of our new methodology is to move from a single-ended to a differential input configuration using a single excitation source for probing a sample, by exploiting the properties of lock-in detection. The advantages of this configuration can be conceptualized by the well-known common-mode rejection which enhances the SNR substantially. In an ideal differential configuration, the output is proportional to the difference between two input signals. If both inputs change level together due to the presence of noise, i.e., a common-mode signal, then the output is not affected at all. Another important advantage is the fact that small amplitude differences between the input channels can be measured, yielding a differential-mode signal. As a result, the sensitivity of the harmonically modulated experiment increases substantially because the differential action suppresses the large background signal, so that the output signal level is of the same order as the contrast signals from a slightly inhomogeneous sample. In what follows, the photothermal or thermal-wave terminology used should be understood to be directly and straightforwardly replaceable by any other periodic signal generation principle that utilizes LIA detection. To remember this important global applicability of the present instrumental methodology, wording referring to the nature of the particular photothermal detection principle will frequently appear in parentheses below.

In order to achieve a differential input with a single excitation source and demodulation instrument, a new periodic optical excitation wave form, Fig. 1(a), has been designed, which exploits advantages due to the built-in weighing-function wave form of the LIA.<sup>3,4</sup> As shown in Fig. 1(a), in a given period  $T$  the sample is excited by two square-wave pulses with center-to-center separation by a time interval  $\Delta$ . As a consequence of the asymmetric periodic excitation, the transient (photothermal) response  $s(t)$  of the sample, Fig.

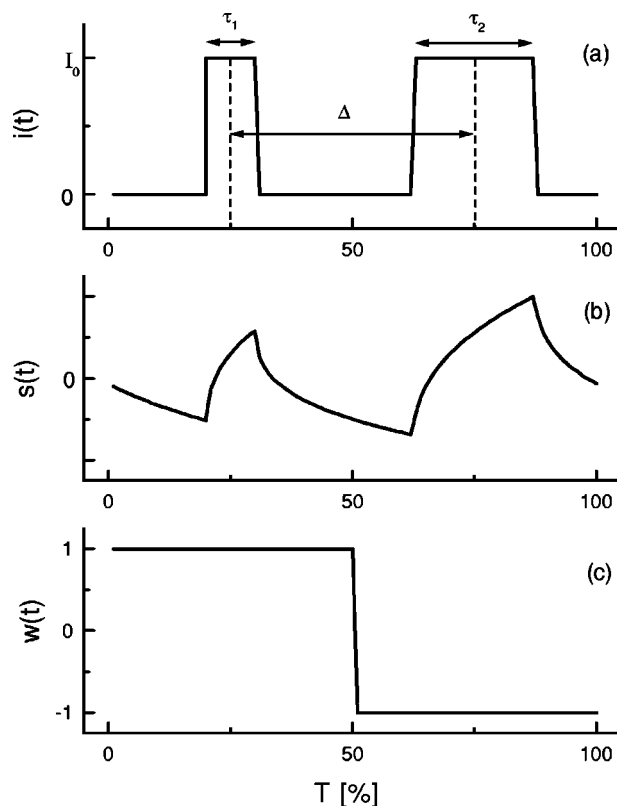


FIG. 1. (a) Optical excitation pulse train  $i(t)$ ; (b) photothermal repetitive transient signal  $s(t)$  due to  $i(t)$ ; (c) lock-in weighing function  $w(t)$ .

1(b), rises and decays twice during a period, also with a certain degree of asymmetry. The actual transient line shapes depend on the signal generation physics. For (photo)thermal-wave detection this line shape depends on the chosen optical excitation wave form and, more importantly, on the thermo-physical properties of the sample. The in-phase or quadrature component of the LIA response to the incoming signal  $s(t)$  with a long integration time constant may be written as<sup>4</sup>

$$y(t) = \int_0^T s(t)w(t)dt = \int_0^{T/2} (+)s(t)dt + \int_{T/2}^T (-)s(t)dt, \quad (1)$$

where  $w(t)$  is the square weighing function shown in Fig. 1(c) and assumed to have a zero-delay rising edge. Owing to the opposite signs of  $w(t)$  across the mid-period point  $T/2$  for zero phase delay at  $t=0$ , the LIA acts like a real-time differential comparator whose output level is a measure of the degree of asymmetry of the two  $s(t)$  line shapes in the two half periods. Therefore, with this wave form design, a differential input configuration is achieved, which suppresses the signal baseline and takes full advantage of the highly efficient noise suppression by the LIA due to its extremely narrow filtering.

The difference between analog and digital LIAs, which use squarewave and synthesized sine-wave reference signals, respectively, has been extensively treated elsewhere.<sup>4</sup> The output is quantitatively the same for the two types of LIA,

provided that a tracking filter is inserted into the input of the analog version, in order to reject the odd harmonics of the input signal.

### III. THEORY OF OUTPUT SIGNAL GENERATION

In this section a theoretical description of the signal generation due to the new wave form of Fig. 1 will be given, providing the expressions for both the in-phase (IP) and quadrature ( $Q$ ) components of the lock-in response. In particular, we are interested in pointing out how the signal output is influenced by the parameters of the composite optical wave form ( $\tau_1$ ,  $\tau_2$ , and  $\Delta$ ), and in studying its sensitivity to the (thermal) response of the sample. In the analysis, we assume that the sample is irradiated with a repetitive optical wave form consisting of two square laser pulses within one period  $T$  having the same intensity  $I_0$ , durations  $\tau_1$  and  $\tau_2$ , and separated by  $\Delta$ . For periodic wave forms it is convenient to consider the Fourier series representation of  $i(t)$

$$i(t) = \sum_{k=-\infty}^{+\infty} c_k \exp\left(\frac{j2\pi kt}{T}\right) \quad (2)$$

in complex form or

$$i(t) = \frac{a_0}{2} + \sum_{k=1}^{+\infty} \left[ a_k \cos\left(\frac{2\pi kt}{T}\right) + b_k \sin\left(\frac{2\pi kt}{T}\right) \right] \quad (3)$$

with

$$c_k = \frac{a_k - jb_k}{2} = \frac{1}{T} \int_{-T/2}^{T/2} i(t) \exp\left(-\frac{j2\pi kt}{T}\right) dt = \frac{1}{T} I\left(\frac{k}{T}\right), \quad (4)$$

where  $I(f)$  is the Fourier transform of  $i(t)$  calculated over one period. By applying the time shift property to the two-square-pulse Fourier transform, it is easy to show that

$$c_k = \left\{ \frac{I_0}{T} \tau_1 \frac{\sin\left(\frac{\pi k \tau_1}{T}\right)}{\frac{\pi k \tau_1}{T}} \exp\left[-j2\pi \frac{k}{T} \left(\frac{T}{2} - \frac{\Delta}{2}\right)\right] \right\} + \left\{ \frac{I_0}{T} \tau_2 \frac{\sin\left(\frac{\pi k \tau_2}{T}\right)}{\frac{\pi k \tau_2}{T}} \exp\left[-j2\pi \frac{k}{T} \left(\frac{T}{2} + \frac{\Delta}{2}\right)\right] \right\} \quad (5)$$

and after some manipulation

$$c_k = \frac{(-1)^k I_0}{\pi k} \left\{ \cos\left(\frac{\pi k \Delta}{T}\right) \left[ \sin\left(\frac{\pi k \tau_1}{T}\right) + \sin\left(\frac{\pi k \tau_2}{T}\right) \right] + j \sin\left(\frac{\pi k \Delta}{T}\right) \left[ \sin\left(\frac{\pi k \tau_1}{T}\right) - \sin\left(\frac{\pi k \tau_2}{T}\right) \right] \right\}. \quad (6)$$

The LIA monitors only the fundamental component of the harmonic signal, so we can limit our attention to the first term of the Fourier series, the coefficients of which are given by

$$c_1 = -\frac{I_0}{\pi} \left\{ \cos\left(\frac{\pi \Delta}{T}\right) \left[ \sin\left(\frac{\pi \tau_1}{T}\right) + \sin\left(\frac{\pi \tau_2}{T}\right) \right] + j \sin\left(\frac{\pi \Delta}{T}\right) \left[ \sin\left(\frac{\pi \tau_1}{T}\right) - \sin\left(\frac{\pi \tau_2}{T}\right) \right] \right\}, \quad (7)$$

$$a_1 = 2 \operatorname{Re}(c_1) = -\frac{2I_0}{\pi} \cos\left(\frac{\pi \Delta}{T}\right) \left[ \sin\left(\frac{\pi \tau_1}{T}\right) + \sin\left(\frac{\pi \tau_2}{T}\right) \right], \quad (8)$$

$$b_1 = -2 \operatorname{Im}(c_1) = \frac{2I_0}{\pi} \sin\left(\frac{\pi \Delta}{T}\right) \left[ \sin\left(\frac{\pi \tau_1}{T}\right) - \sin\left(\frac{\pi \tau_2}{T}\right) \right]. \quad (9)$$

In order to calculate the LIA response to the excitation pulse train, we introduce the photothermal frequency response  $S(f) = \operatorname{Re}[S(f)] + j \operatorname{Im}[S(f)]$ , which can be unambiguously defined for each sample as the Fourier transform of the transient photothermal impulse response. In so doing, the LIA output may be written as

$$Y(f) = \{[\operatorname{Re}[S(f)] + j \operatorname{Im}[S(f)]](a_1 + jb_1)\}, \quad (10)$$

which can be eventually decomposed into IP and  $Q$  components given by

$$Y_{\text{IP}} = \operatorname{Re}[Y(f)] = -\frac{2I_0}{\pi} \left\{ \cos\left(\frac{\pi \Delta}{T}\right) \left[ \sin\left(\frac{\pi \tau_1}{T}\right) + \sin\left(\frac{\pi \tau_2}{T}\right) \right] \operatorname{Re}[S(f)] + \sin\left(\frac{\pi \Delta}{T}\right) \left[ \sin\left(\frac{\pi \tau_1}{T}\right) - \sin\left(\frac{\pi \tau_2}{T}\right) \right] \operatorname{Im}[S(f)] \right\} \quad (11)$$

and

$$Y_Q = \operatorname{Im}[Y(f)] = \frac{2I_0}{\pi} \left\{ \sin\left(\frac{\pi \Delta}{T}\right) \left[ \sin\left(\frac{\pi \tau_1}{T}\right) - \sin\left(\frac{\pi \tau_2}{T}\right) \right] \operatorname{Re}[S(f)] - \cos\left(\frac{\pi \Delta}{T}\right) \left[ \sin\left(\frac{\pi \tau_1}{T}\right) + \sin\left(\frac{\pi \tau_2}{T}\right) \right] \operatorname{Im}[S(f)] \right\}. \quad (12)$$

It can be seen that, in order to obtain a true differential output, the pulse widths *must be different*. Otherwise, the effect of the new optical wave form is only to generate a signal equivalent to that obtained from the conventional frequency scan method, from which it differs only by a multiplicative (amplitude) factor. This is physically reasonable, because the effect of two equal-width pulses is the same in the two half periods, Fig. 1, and as a result it does not reveal the asymmetric behavior of the response  $s(t)$ . If  $\tau_1$  is different from  $\tau_2$ , then the mixer-low-pass filter action of the LIA mixes the IP- and  $Q$ -channel signals created by the single-ended or by the equal-width two-pulse wave form. It is most interesting that the demodulated signal output multiplication factors are the real and the imaginary part of the (photothermal) response  $S(f)$ .

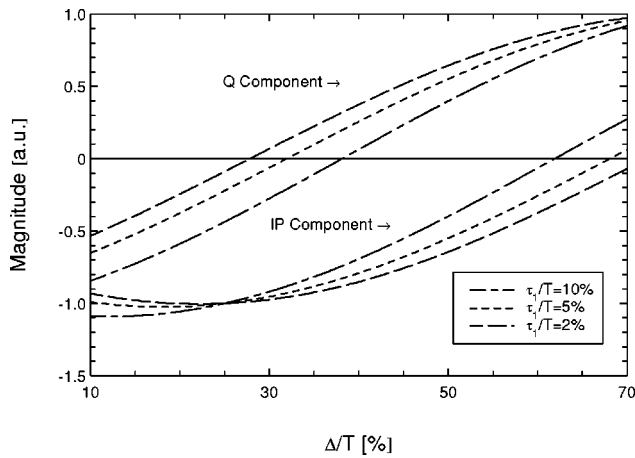


FIG. 2. Amplitude of the IP and  $Q$  component of the LIA response, as function of the separation between two pulses calculated from Eqs. (11) and (12), respectively, for the  $\tau_1/T$  values reported in the inset. The sample has been assumed homogeneous, i.e.,  $\text{Re}[S(f)] = -\text{Im}[S(f)]$  and  $\tau_2/T = 25\%$ .

As a simple example, we recall that the one-dimensional photothermal frequency response of an ideally homogeneous sample is given by<sup>1</sup>

$$S(f) = A \frac{I_0}{\sqrt{k\rho c}} \frac{(1-j)}{\sqrt{f}}, \quad (13)$$

where  $A$  is a constant depending on the experimental geometry; and  $(k\rho c)^{0.5}$  is the thermal effusivity of the sample, where  $k$ ,  $\rho$ , and  $c$  are, respectively, the thermal conductivity, the density and the specific heat. The real and the imaginary parts of the response  $S(f)$  have the same absolute magnitude for a homogeneous sample. It is then possible to balance the two terms in the IP and  $Q$  components for appropriate values of  $\tau_1$ ,  $\tau_2$ ,  $\Delta$ , so as to obtain zero magnitude for either the IP or the  $Q$  signal channel. Figure 2 shows the theoretical behavior of the IP and  $Q$  channel outputs obtained from a homogeneous sample as a function of the pulse separation  $\Delta$  for different  $\tau_1/T$  values. The plots clearly show the existence of particular pulse separation values  $\Delta_{0,IP}$  and  $\Delta_{0,Q}$  for which the IP or the  $Q$  component is equal to zero.

Modifying the (thermophysical or geometrical) properties of the sample leads to different values of the ratio  $\text{Re}[S(f)]/\text{Im}[S(f)]$ , thus shifting the output zero to a new position along the  $\Delta$  axis. The IP and  $Q$  loci of the zero crossing points can be derived from Eqs. (11) and (12), and are given by the following expressions:

$$\tan\left(\frac{\pi\Delta_{0,IP}}{T}\right) = \left\{ \frac{\text{Re}[S(f)]}{\text{Im}[S(f)]} \frac{\sin\left(\frac{\pi\tau_1}{T}\right) + \sin\left(\frac{\pi\tau_2}{T}\right)}{\sin\left(\frac{\pi\tau_2}{T}\right) - \sin\left(\frac{\pi\tau_1}{T}\right)} \right\} \quad (14)$$

and

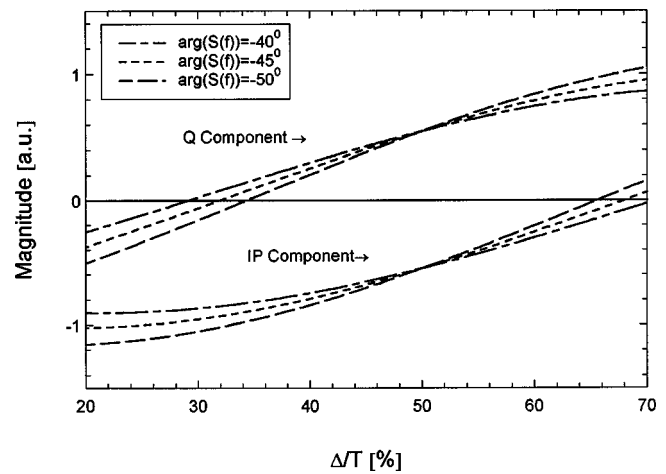


FIG. 3. Amplitude of the IP and  $Q$  component of the LIA response, as a function of the pulse separation, for different argument of  $S(f)$  reported in the inset.  $\tau_1/T$  and  $\tau_2/T$  have been assumed equal to 5% and 25%, respectively.

$$\tan\left(\frac{\pi\Delta_{0,Q}}{T}\right) = \left\{ \frac{\text{Im}[S(f)]}{\text{Re}[S(f)]} \frac{\sin\left(\frac{\pi\tau_1}{T}\right) + \sin\left(\frac{\pi\tau_2}{T}\right)}{\sin\left(\frac{\pi\tau_1}{T}\right) - \sin\left(\frac{\pi\tau_2}{T}\right)} \right\}. \quad (15)$$

The existence of zeros in the outputs appears promising, because information about the degree of thermal homogeneity of a given sample over a depth determined by the thermal diffusion length, can be readily obtained from the position of the zero on the  $\Delta$  axis for different values of  $\tau_1$  or  $\tau_2$ . This leads to several advantages over the conventional (photothermal) measurement methodologies. First, it is no longer necessary to compare the signal with that from a homogeneous reference sample, thus avoiding the SNR deterioration problems mentioned earlier. Moreover, in principle, the position of the zero is not affected by the pump beam intensity. Therefore, for direct thermophysical comparisons between different samples, it is no longer required to run the experiment with exactly the same intensity as required for the conventional 50% duty-cycle frequency-scan method. If this condition is not fulfilled, then the amplitude ratio is affected by a hard-to-estimate multiplication factor, and it can no longer be used for quantitative measurements of the sample properties. The insensitivity of the double-repetitive-pulse-generated LIA signal channel outputs to incident optical intensity further leads to the conclusion that random fluctuations of the intensity, which normally are not suppressed by LIA filtering,<sup>2</sup> affect less the response of the experiment (a “common-mode rejection”; see Part II of this work<sup>5</sup>). Of course, an additional noise suppression factor in this technique is the constant, single-frequency bandwidth used for the entire measurement.<sup>6</sup> This substantially limits the noise output compared to the variable bandwidth of a conventional frequency or time scan<sup>7</sup> and is an instrumental feature commonly shared with the single pulsedwidth-scan LIA method.<sup>8</sup>

In Fig. 3 both the IP and  $Q$  amplitude, calculated according to Eqs. (11) and (12), are shown as functions of the pulse separation for  $\tau_1/T = 5\%$ ,  $\tau_2/T = 25\%$ , and for different



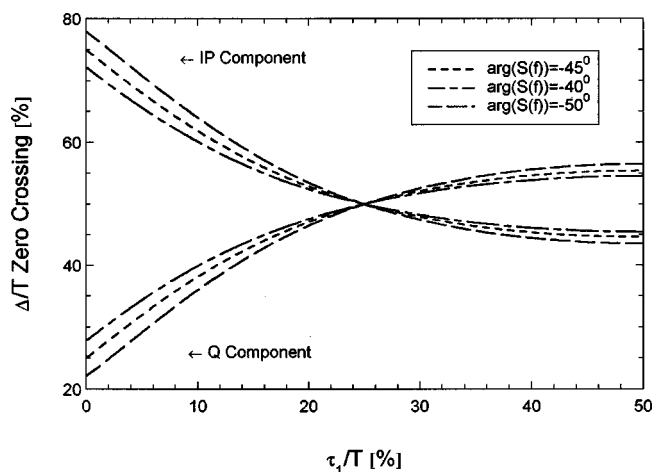


FIG. 4. Dependence of the zero crossing values  $\Delta_{0,IP}$  and  $\Delta_{0,Q}$  on the duration of the first pulse for the  $\arg[S(f)]$  values reported in the inset.  $\tau_2/T$  has been assumed to be equal to 25%.

$\text{Im}[S(f)]/\text{Re}[S(f)]$  ratios corresponding to the  $\arg[S(f)]$  values reported in the inset. The  $Q$  component crosses the zero amplitude axis at lower values of  $\Delta$  than the IP component. This can be understood in terms of the fact that the *odd*  $w(t)$  weighing function used at the mixing stage to obtain the  $Q$  component is the one actually shown in Fig. 1(c). The *even* weighing function used to obtain the IP component is shifted by  $T/2$ , which implies an equivalent shift of the zero positions close to the upper edge of the  $\Delta T$  axis.

Figure 4 shows the locus of zeroes as a function of  $\tau_1$  for  $\tau_2/T = 25\%$  and for the  $\arg[S(f)]$  values shown in the inset. It is seen that the greater the difference in value between pulse widths  $\tau_1$  and  $\tau_2$ , the better the loci positions are resolved. This reflects, again, the fact that the use of two different pulse widths forces the (photothermal) response to show a measurably different behavior in the two half periods which, in turn, amplifies inhomogeneity-generated responses from a sample. These facts corroborate the use of narrow pulsewidths. Long pulse widths limit the available  $\Delta$  scan range and hence the resolution of the experiment.

In Fig. 5 both the IP and  $Q$  components are reported as a function of the pulse separation for different values of the sample effusivity reported in the inset. Of course the crossing position is not affected because a change in the effusivity does not change the  $\text{Im}[S(f)]/\text{Re}[S(f)]$  ratio in the simple case of Eq. (13). Nevertheless, the slopes of the theoretical curves near the crossing point show a clear dependence on this thermophysical parameter. This means this technique

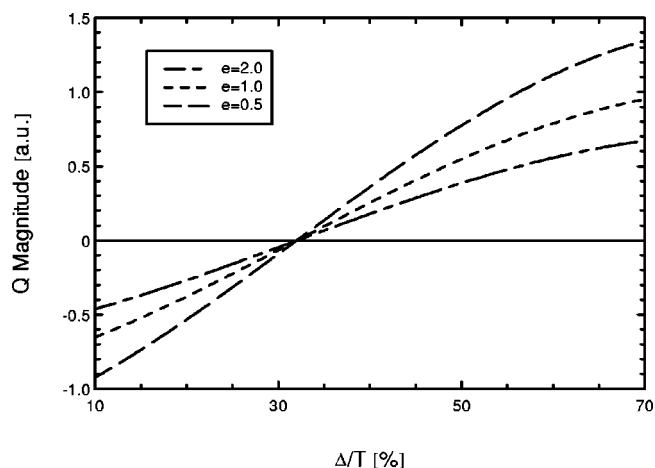


FIG. 5. Amplitude of the  $Q$  component, as a function of the pulse separation, calculated according to Eqs. (11) and (12) for the thermal effusivity values reported in the inset (in units of  $\text{ws}^{1/2}/\text{cm}^2 \text{ K}$ ). The sample has been assumed homogeneous;  $\tau_1/T$  and  $\tau_2/T$  are equal to 5% and 25%, respectively.

can be applied just as well on thermally homogeneous samples in order to compare their thermal effusivity.

In conclusion, the novel common-mode rejection LIA pulse wave form offers adequate flexibility to design an experiment suitably optimized so as to interrogate minute (thermal) inhomogeneities in a sample, by effectively suppressing the background signal and simultaneously monitoring any shift in the demodulated output zero-amplitude position from that of a homogeneous reference.

## ACKNOWLEDGMENTS

The authors would like to acknowledge the support of the Natural Sciences and Engineering Research Council of Canada (NSERC) and Materials and Manufacturing Ontario (MMO).

<sup>1</sup> See, for example, G. Busse and H. G. Walther, in *Progress in Photothermal and Photoacoustic Science and Technology*, Vol. I: Principles and Perspectives of Photothermal and Photoacoustic Phenomena, edited by A. Mandelis (Elsevier, New York, 1992), Chap. 5, pp. 207–298.

<sup>2</sup> C.-H. Wang and A. Mandelis, *Rev. Sci. Instrum.* (in press).

<sup>3</sup> G. L. Miller, J. V. Ramirez, and H. A. Robinson, *J. Appl. Phys.* **46**, 2638 (1975).

<sup>4</sup> A. Mandelis, *Rev. Sci. Instrum.* **65**, 3309 (1994).

<sup>5</sup> S. Paoloni, L. Nicolaides, and A. Mandelis, *Rev. Sci. Instrum.* **71**, 2445 (2000).

<sup>6</sup> J. Shen, A. Mandelis, and B. D. Aloysius, *Int. J. Thermophys.* **17**, 1241 (1996).

<sup>7</sup> M. Munidasa and A. Mandelis, *Rev. Sci. Instrum.* **65**, 2344 (1994).

<sup>8</sup> A. Mandelis and M. Munidasa, U.S. Patent 5,667,300 (September 16, 1997).